JSAE 201109044
SAE 2011-01-2001

# Influence of injection strategy in a high-efficiency hydrogen direct injection engine

**Thomas Wallner, Nicholas S. Matthias, Riccardo Scarcelli**
Argonne National Laboratory

Copyright © 2011 Society of Automotive Engineers of Japan, Inc.

## ABSTRACT

Energy security and climate change are two of the main drivers for development of sustainable and renewable transportation solutions. Entities around the globe have been working on strategic plans to reduce energy consumption and curb greenhouse gas emissions. In this context hydrogen is frequently mentioned as the fuel and energy carrier of the future. The U.S. Department of Energy's (DOE's) FreedomCAR and Vehicle Technologies (FCVT) Program has identified hydrogen-powered internal combustion engine (ICE) vehicles as an important mid-term technology on the path to a large-scale hydrogen economy. DOE has set challenging goals for hydrogen internal combustion engines including 45% peak brake thermal efficiency (BTE).

This paper summarizes recent research engine test results employing hydrogen direct injection with different injection strategies. A dedicated research engine optimized for lean hydrogen operation with a compression ratio of 12.9:1 was built and fast-acting Piezo injectors are used for the test sequence. Turbocharged high-load conditions are analyzed at several engine speeds to provide a full spectrum of relevant engine results for achieving peak efficiencies. Three injector nozzle designs are experimentally tested for their ability to meet the 45% efficiency target and their implication on engine-out $NO_X$ emissions. Complimentary to experimental work 3-D CFD simulation is employed to analyze the mixture formation process and predict the ability of newly designed nozzles to provide favorable charge stratification.

The result of this integrated approach is a combustion system that is capable of achieving high engine efficiencies while minimizing the $NO_X$ emissions penalty. Peak indicated efficiencies of 46-47% were reached at full load conditions translating into peak brake thermal efficiencies of approx. 45%. At the same time engine-out $NO_X$ emissions below 200 ppm could be maintained with certain operating conditions reaching $NO_X$ levels below 100 ppm.

## INTRODUCTION

Hydrogen internal combustion engines ($H_2$-ICEs) have been studied for decades as a promising approach to reduce harmful emissions from vehicles while meeting the required performance in terms of power output [1,2,3]. In particular, direct injection of hydrogen (DI-$H_2$) has the potential to achieve high power density while reducing the risk for combustion anomalies compared to a more conventional hydrogen port-fuel injection (PFI) strategy [4]. Research projects on DI $H_2$-ICEs, funded by the DOE since 2005, target ambitious goals including the same power density as comparable gasoline engines, 45% peak BTE and $NO_X$ emissions as low as 0.07 g/mile [5].

A research group at Argonne National Laboratory has been focusing on developing advanced direct injection strategies on a single-cylinder $H_2$-ICE [6,7] with the goal of increasing engine efficiency by optimizing mixture formation and combustion processes. A recent upgrade of the single-cylinder geometry, consisting of increasing compression ratio and engine stroke, aimed at achieving higher theoretical efficiencies. In addition, the replacement of the solenoid-operated injection system with an improved piezo-actuated system allowed for delivering much higher quantities of hydrogen in the same amount of time [8]. This upgrade also extended the operating envelope to higher engine speeds and loads which is expected to further increase the peak BTE.

The proper injection timing is a key-factor in DI engines and improvements in engine efficiency can be achieved by optimizing the start of injection (SOI) for every condition of engine load and speed. In this paper, the analysis of the influence of engine speed and SOI on the mixture stratification and combustion, and thus on the engine efficiency, is reported. The main focus of this study is on turbocharged operating conditions which result in increased power and BTE and also present the most critical scenario for $NO_X$ emissions. The analysis includes three injector configurations and highlights the significant influence of the nozzle geometry on the mixture formation process. This paper extends the range of operation of

previous work [8] and represents a comprehensive analysis and useful baseline for further optimization of engine parameters and nozzle geometries in engines employing direct injection of a gaseous fuel.

In addition to extensive experimental activities, 3-D CFD simulations were performed to gain insight into the physics involved in the mixture formation process of $H_2$ DI-ICEs. A commercial CFD code was used to provide an accurate description of the injection and mixture formation process. Numerical results aim at supporting experimental work and providing guidelines for further engine optimization, allowing innovative geometries to be evaluated within hours and thus drastically reducing the test time and cost of prototypes.

## BACKGROUND

In order to optimize the efficiency of hydrogen internal combustion engines ($H_2$-ICEs), it is crucial to analyze the major factors influencing the engine efficiency and the related loss mechanisms. Analysis of losses is a means of identifying individual losses that can be attributed to factors influencing efficiency. The analysis starts with a thermodynamic model of the engine cycle which is used to calculate the efficiency of the ideal engine with real charge. From that, the following series of losses are subtracted to derive the actual indicated thermal efficiency (ITE) of the engine: injection during compression stroke ΔICS, incomplete combustion ΔIC, real combustion ΔRC, wall heat losses ΔWH, and gas exchange losses ΔGE. The efficiency of the ideal engine with real charge is defined as the theoretical efficiency achievable using measured fuel and air mass while assuming constant volume combustion at TDC, indefinitely short fuel injection at TDC as well as adiabatic processes. The loss due to injection during the compression stroke considers non-ideal injection with actual start of injection (SOI) and finite injection duration. Incomplete combustion accounts for the unburned fuel, which is measured using a hydrogen sensor in the exhaust. The losses due to real combustion account for the actual combustion process with a finite duration as well as phasing different from TDC. Finally, losses due to heat transfer to the cylinder walls during combustion as well as gas exchange are calculated.

Previous work on the single-cylinder $H_2$-ICE at Argonne National Laboratory was aimed at improving the engine efficiency by upgrading the geometry [8]. The upgraded engine compared to its predecessor features an increased compression ratio along with a decreased bore/stroke ratio (see Table 1). ITE improved by approximately 6% over the previous engine configuration and a detailed analysis of the partial losses showed that the increase was mainly due to higher theoretical efficiencies and reduced wall heat losses. With the upgraded engine, an ITE of 43.0% was demonstrated for the engine under naturally aspirated conditions (2000 RPM, 8 bar IMEP) and a peak ITE of 45.6% was achieved under turbocharged conditions (3000 RPM, 14.3 bar IMEP). These results also suggest that the DOE target of 45% peak brake thermal efficiency is within reach and can be achieved through minimizing each of the above-mentioned losses. Progress documented in [8] provides a foundation for the current work, aimed at further improving efficiency by studying the effects of injection strategy and injector nozzle geometry.

**Table 1: Research engine geometry**

| | |
|---|---|
| Displacement [L] | 0.66 |
| Bore/stroke [mm] | 89/105.8 |
| Bore/stroke ratio [-] | 0.84 |
| Compression ratio [-] | 12.9 |
| Intake valve timing | IVO = 15 °CA BTDC<br>IVC = 35 °CA ABDC |
| Exhaust valve timing | EVO = 45 °CA BBDC<br>EVC = 10 °CA ATDC |
| Injector actuation | Piezo |

To enable optimization of injection strategy, an advanced fuel delivery system equipped with a piezo-actuated injector was tested. The specific injector used was a prototype injector provided by Westport Innovations, Inc. Faster acting piezo-injectors with higher mass flow rates allow greater flexibility in terms of injection strategy because the injection duration is shorter than with the previous generation of solenoid injectors. Thus, the engine can be operated at higher speeds and loads and the injection can start later in the compression stroke. The evident benefit of a late SOI is the reduction of the compression work.

The potential for efficiency improvement due to later injection has previously been assessed [3,9]. Figure 1 shows the theoretical losses due to injection during the compression stroke as a function of both SOI and air fuel ratio. Injection duration and compression ratio are held constant at 40 °CA and 10.5 respectively. Losses decrease with later SOI and reduced amount of injected fuel represented as increased air fuel ratio. The plot suggests that at λ=2 the losses decrease by approximately 0.2% if SOI is delayed from 140 °CA BTDC to 120 ° CA BTDC and by another 0.4% if SOI is further delayed to 100 °CA BTDC.

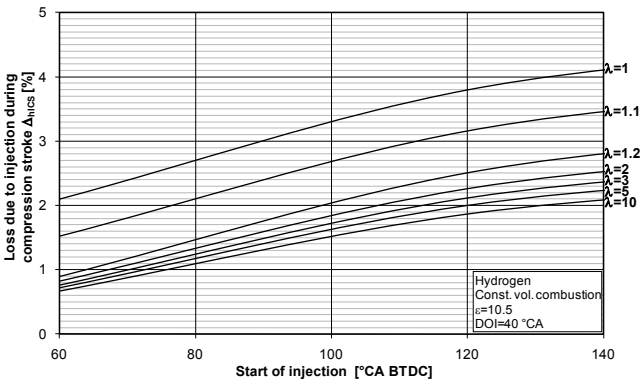


**Figure 1: Theoretical losses due to injection during the compression stroke [9]**

Nevertheless, delaying the start of injection also affects the mixture formation process. Another effect of a late SOI is an increase in mixture stratification. Delayed SOIs provide a shorter time for the fuel jet penetration within the combustion chamber and proper mixing with air. With insufficient time for complete mixing, part of the charge may be

stoichiometric or even rich at ignition timing even though the global equivalence ratio is lean (typical values of equivalence ratio in this study are $\phi \sim 0.4/\lambda \sim 2.5$). However, a proper stratification of the mixture around the spark plug at the ignition time can increase the combustion efficiency (rich mixture close the spark plug) while maintaining low losses due to wall heat transfer (ultra-lean mixture close to the cylinder walls). This research focuses on how to take advantage of the mixture stratification due to direct injection of hydrogen during the compression stroke and analyzes the effect on individual losses as well as $NO_X$ formation.

Incomplete combustion accounts for hydrogen that leaves the cylinder without participating in the combustion reaction. Major sources determining the amount of unburned fuel include the crevice volume between the piston and cylinder walls, mixtures outside $H_2$ flammability limits, and flame quenching close to the combustion chamber walls. In general $H_2$ has wide flammability limits, defined by equivalence ratios between $0.1 < \varphi < 7.1$ ($10 > \lambda > 0.14$) [3]. Ideal mixture stratification would provide mixtures within the $H_2$ flammability limits and negligible amount of $H_2$ close to the walls or trapped in the crevice volume in order to avoid incomplete combustion.

Losses due to real combustion account for the fact that the combustion process is not instantaneous. In the ideal engine it is assumed that constant volume combustion occurs at TDC, which is not physically possible. The amount of time required for combustion depends on many factors including the flame speed which is largely a function of equivalence ratio. In general, rich mixtures burn more quickly than lean mixtures [4]. Accordingly, faster reactions (i.e. richer mixtures) will minimize the loss due to real combustion. Therefore, as above-mentioned, ideal mixture stratification would have a rich mixture close to the spark plug which rapidly develops the first flame kernels and spreads the flame front throughout the combustion chamber. Another important factor in the analysis of losses due to real combustion is the combustion phasing. If one does not consider wall heat losses, the ideal phasing of the combustion would be symmetrical around TDC. However, taking wall heat losses into account a combustion phasing with a 50% mass fraction burned (MFB) location around 8°CA ATDC is widely considered optimal.

Wall heat losses account for heat transfer from the in-cylinder gases to the cylinder walls. The driving force is the temperature gradient between the combustion gases and the cylinder walls. In other words, high temperature gases in close proximity to the walls result in high heat transfer. Measurements of wall heat transfer on a hydrogen engine suggest that disadvantageous mixture stratification results in a non-linear increase in local wall heat transfer [9]. Furthermore, due to the shorter quenching distance, wall heat losses with hydrogen are potentially increased compared to gasoline operation. Assuming the highest temperature gases are those resulting from rich $H_2$ combustion, ideal mixture stratification would avoid rich mixtures close to the cylinder walls.

In order for hydrogen engines to be a considered a viable solution they must meet the most stringent $NO_X$ emissions regulations preferably without after-treatment systems. To this aim it is important to understand the effect of mixture stratification on $NO_X$ emissions. Homogeneous $H_2$ combustion is a good point of reference for evaluating $NO_X$ emissions. Figure 2 shows the $NO_X$ emissions trend for homogeneous lean operation as a function of equivalence ratio. From this trend it is obvious that lean $H_2$ combustion produces very little $NO_X$ and there is a critical equivalence ratio where $NO_X$ increases greatly. The critical level is approximately $\phi = 0.5$ ($\lambda = 2$), where a sharp increase in $NO_X$ followed by a decrease approaching stoichiometric combustion can be observed [4]. Applying this knowledge to stratified combustion, an overall lean mixture ($\phi < 0.5$) with rich pockets ($\phi > 1.0$) is expected to be beneficial in terms of $NO_X$, compared to a homogeneous mixture at $\phi \sim 0.75$.

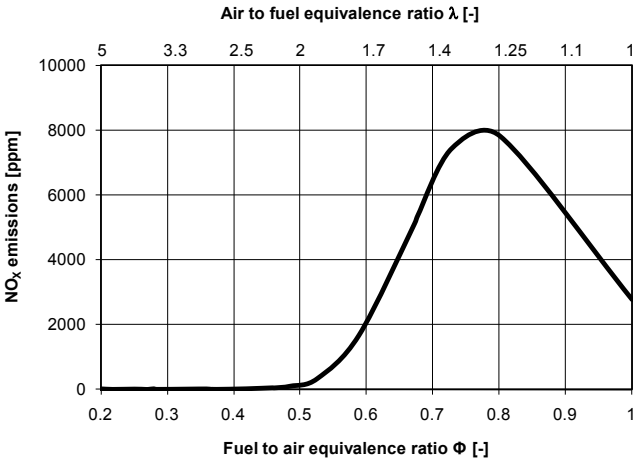


**Figure 2: $NO_X$ emissions trend for homogeneous $H_2$ combustion [4]**

Overall, $H_2$-ICEs show great potential to meet the efficiency and emissions targets set forth by DOE. Improved engine geometry and fast-acting piezo-actuated injectors have shown promising results in previous work [8]. With this foundation a considerable effort is being made to optimize the injection strategy with specific focus on mixture stratification. Ideal mixture stratification has been conceptualized and the approach to achieving such stratification through an iterative process including design, assessment employing 3D-CFD simulation and experimental testing of different injector nozzles is summarized in this paper.

## NUMERICAL AND EXPERIMENTAL DETAILS

### 3-D CFD SIMULATION

This paper includes CFD results on direct injection of hydrogen in addition to experimental results, in order to provide further insight in the processes occurring within the combustion chamber during the mixture formation and compression stroke. Details on the numerical approach employed in this study have already been published [10] and are only briefly discussed here. In this work, numerical simulations

focus on direct injection during the compression stroke, thus only a portion of the actual engine geometry (including combustion chamber and nozzle configuration) is considered and only a fraction of the engine cycle (from IVC to TDC) is analyzed. Nevertheless, the flow field and the main physical quantities at IVC (initial conditions) are taken into account and are the result of previous calculations which are not reported here. Such conditions are likely to be stable at a fixed engine speed and load, since conditions in the intake and exhaust zones are mostly unvaried and the injection timing (SOI) or the nozzle geometry has no significant effect on the in-cylinder pressure at EVO. Previous work [10] validated the flow-field numerical predictions against experiments in terms of PIV data in a similar, but optically accessible, engine.

With the geometry defined and initial conditions being known, the only information which has to be set as input to the computational code is the injection profile, which is calculated on the basis of experimental data (mass of fuel injected and injection duration) with the assumption of a trapezoidal injection law. This approach has demonstrated the capability to accurately simulate jet penetration (quantitatively) and air/fuel mixing (qualitative) based on the validation against optical data [10,11]. Simulating injection in this way has been proven effective in previous work as it was used to improve the analysis of engine performance and highlight the effect of injection timing and nozzle configuration on mixture formation [8].

## NOZZLE DESIGN AND GEOMETRY

A schematic view of the combustion chamber of the single-cylinder research engine used for this study is shown in Figure 3. The injector is placed in a central location close to the spark plug, although its location is not perfectly symmetric with respect to the cylinder. The schematic also shows the injector protrusion and its location relative to the spark plug on a vertical plane through the injector and spark plug axes.

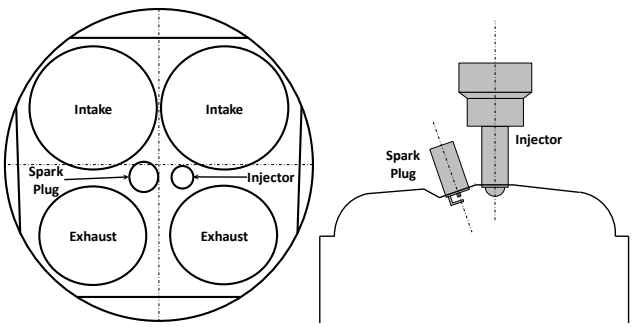


**Figure 3: Schematic of the research engine geometry**

The central location of both injector and spark plug presents a challenging scenario for optimizing mixture formation through design of injector nozzle and injection sequence. Under these boundary conditions properly stratifying the gaseous jet around the spark plug is not trivial. It is worth noting that for the majority of results presented in this study a hydrogen injection pressure of 100 bar was used. Such a pressure results in supersonic jets with velocities downstream of the nozzle in the order of 1250 to 2500 m/s (in the under-expanded region Ma >> 1). Accordingly, even with directing the hydrogen jet directly towards the spark plug it is not possible to localize most of the hydrogen around the spark plug at ignition timing.

**Table 2: Injector nozzles specifications**

| Nozzles Configuration | | | |
|---|---|---|---|
| Number of holes | 5 | 13 | 2 |
| Injection angle (°) | 35 | 30 | 70 |
| Hole diameter (mm) | 0.61 | 0.313 | 1 |
| Total flow area ($mm^2$) | 1.48 | 1.00 | 1.57 |
| Instant. $H_2$ mass flow (at 100 bar) (g/s) | 5.83 | 4.57 | 6.87 |
| Inj. duration (3000 RPM 14bar IMEP) (°CA) | 54.5 | 67 | 47 |

Thus, the choice of the nozzle geometry is a consequence of the injection strategy, which can provide jets impinging the piston, the cylinder walls or spreading throughout the combustion chamber. Three different nozzles were designed and tested in this study, characterized by 2, 5 and 13 holes (Figure 4). Main specifications of the nozzle geometries are provided in Table 2. A previous study used a 5-hole injector to provide a homogeneous mixture at ignition timing with early injection (SOI=140°CA) [8]. The 2-hole and 13-hole nozzles were subsequently designed with the goal either to increase the mixture stratification (2-hole) or to increase the air entrainment in the hydrogen jets (13-hole).

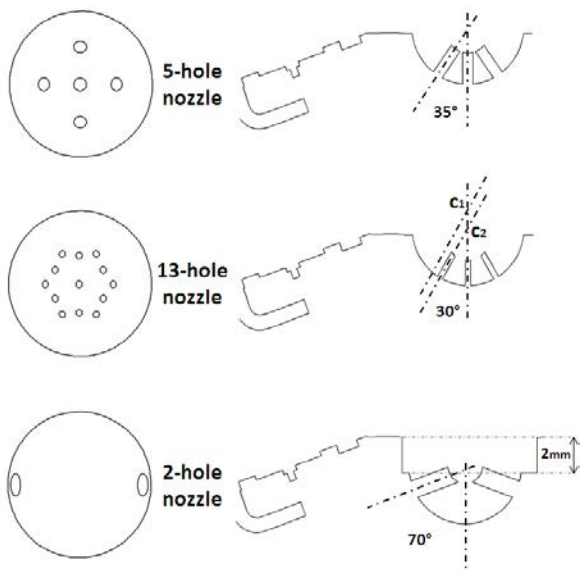


**Figure 4: Schematic geometries of the examined injector nozzles**

The 13-hole nozzle was designed with a central hole and 12 holes at 30° angle with respect to the vertical and with a zig-zag distribution due to the different location of the rotation center (see Figure 4). This nozzle was expected to show strong jet-to-jet interaction which ultimately resulted in a single jet aiming towards the piston (Figure 5). The 2-hole nozzle was designed with a significantly wider angle with respect to the vertical (70°) and without central hole for two main reasons. First, any possible interaction between the jets is avoided, furthermore the effect of a different strategy (jet impinging the cylinder walls and interacting with the piston as it

approaches TDC) can be evaluated. Figure 4 also shows that the injector protrusion with the 2-hole nozzle is increased (by about 2 mm) in order to reduce the impingement and interaction of the supersonic jets with the pent-roof and the spark plug. Preliminary results showed that this phenomenon might slow the jets down immediately at the nozzle exit decreasing the jet penetration and leading to unstable operation characterized by high COV.

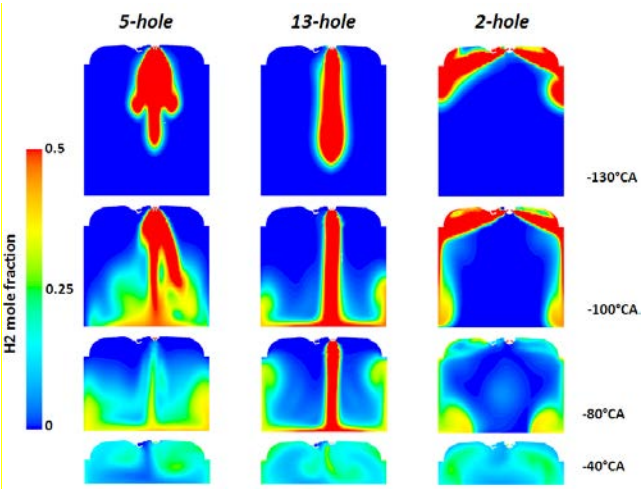


**Figure 5: Jet development and mixture formation process with different nozzle designs (SOI = 140°CA)**

A preliminary CFD assessment of hydrogen jet development and the mixture formation processes for the different injector nozzle geometries is shown in Figure 5. The figure shows the hydrogen mole fraction for several time steps during the compression stroke with hydrogen rich zones in red and zones of air in blue. The images clearly show the differences in progression of the jets starting shortly after SOI until the end of the compression stroke. Although the 5-hole nozzle shows distinct jets right after the start of injection the angle between the jets is reduced due to jet-to-jet interaction which ultimately results in one main jet aimed at the piston. This effect is even more pronounced for the 13-hole injector where all jets collapse into one immediately at the nozzle exit. The phenomenon is referred to as Coanda Effect [12], and it is caused by the lack of air entrainment within the gaseous jet. When this happens, the jet deviates towards the region with less air entrainment. As a consequence of the nozzle symmetry, all jets deviate towards the central jet and subsequently merge into a single jet. Conversely, the 2-hole injector, due to the wider injection angle, provides two distinct jets that impinge on the combustion chamber walls before hitting the piston during its upward motion. It is clear from Figure 5 that regardless of nozzle design an ignitable mixture around the spark plug develops at ignition timing, suggesting stable operation with this early injection strategy (SOI=140°CA BTDC). The vast differences in fuel distribution throughout the combustion chamber highlight the influence of the nozzle configuration. These differences, as mentioned above, underline the importance of a proper design of the injection strategy including nozzle design as well as injection sequence. As mentioned earlier, numerical simulations consider the actual flow conditions in the combustion chamber, so that the influence of intake flow on mixture formation can be taken into account. Mixture formation is certainly affected by the in-cylinder tumble (in this case) motion, although a significant effect is expected only during late compression, when the orders of magnitude of jet velocity and flow velocity become comparable. Accordingly, especially at high engine speed, optimized jet direction can be the key to postpone the SOI, thus reducing the compression work and increasing the engine efficiency.

## OPERATING CONDITIONS

Each of the three injectors shown in Figure 4 was tested using engine operating conditions slightly above the typical full load curve of a naturally aspirated gasoline engine. The engine was run in turbocharged, lean operating condition at three different speeds typical for light duty engines; 2000, 2500, and 3000 RPM. Turbocharging was simulated by supplying boosted intake air from an external air compressor. Using PID controlled intake and exhaust pressure valves, an intake pressure of 2 bar and an exhaust pressure of 1.8 bar were maintained. The fueling was controlled to maintain a constant equivalence ratio $\phi = 0.4$ ($\lambda = 2.5$) resulting in different injection durations for each injector (see Table 2). The nominal load was approximately 14.5 bar IMEP, which changed slightly as a function of engine speed.

Two uncooled high-speed pressure transducers were used simultaneously to acquire crank angle resolved in-cylinder pressure data (AVL GG22C). Having two transducers in parallel allows the pressure data to be cross checked for accuracy. Steady state data was acquired during a 30 second window in each case which equates to 750 engine cycles at 3000 RPM, 625 at 2500 RPM, and 500 at 2000 RPM. IMEP values used for calculating engine efficiency were derived using the average pressure data within the 30 second window. Other values reported ($NO_X$, $\lambda$, etc.) are also 30 second averages acquired at the same time as the corresponding pressure data. The other critical parameter for calculating engine efficiency is the fuel mass. Hydrogen mass flow to the engine was measured using a coriolis flow meter (Micro Motion CMF010P). The reported data points for the SOI sweeps are the average of three samples at that operating condition and the standard deviation between iterations is around 0.05% for ITE and 6 ppm for $NO_X$, approximately the width of the data markers in the plot (with the exception of late SOI cases where engine operation is less stable).

An SOI sweep was performed in each case starting with an early SOI where the mixture is expected to be relatively homogeneous. The nominal start of injection for early SOI is 140°CA BTDC which is just after intake valve closing. SOI was then progressively delayed until stable combustion could no longer be sustained. Stability of the combustion was assessed using the coefficient of variation of the indicated mean effective pressure as a threshold ($COV_{IMEP} < 5\%$). Maximum brake torque (MBT) ignition timing was used in all cases, generally resulting in a 50% mass

fraction burned (MFB) location around 8°CA ATDC, the same optimal combustion phasing that was reported in previous work on this engine [8].

## RESULTS

As outlined earlier the test program included SOI sweeps at three engine speeds with three different injector nozzles. In addition the influence of injection pressure was evaluated using pressures of 100 and 140 bar. In all cases the injection strategy was limited to a single injection during the compression stroke. Results show the influence of the nozzle design on mixture stratification and subsequently combustion, efficiency and emissions at the highest tested engine speed of 3000 RPM followed by an analysis of the influence of engine speed. Results include 3D-CFD mixture stratification at ignition timing and measured pressure traces as well as derived information including rates of heat release (ROHR) and a detailed analysis of losses for relevant operating conditions. Finally the different nozzles are compared based on efficiency and $NO_X$ emissions measurements. In this paper, the numerical results are shown in two orthogonal vertical planes through the spark plug as well as the horizontal plane corresponding to the fire-deck (Figure 6).

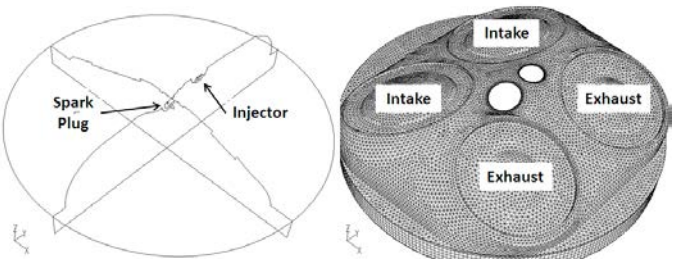


**Figure 6: Schematic of the data planes and their position with respect to the intake and exhaust regions**

INFLUENCE OF NOZZLE DESIGN

5-hole nozzle

The distribution of hydrogen at MBT ignition timing as a function of SOI for the 5-hole nozzle can be seen in the CFD results shown in Figure 7. The scale reports both air fuel ratio ($1 < \lambda < 4$) and equivalence ratio ($0.25 < \phi < 1$), with leaner mixtures represented in blue and stoichiometric mixtures in red. For the SOI 140°CA BTDC case a relatively rich mixture is present towards the intake side of the combustion chamber as well as in close proximity to the injector. However, the area around the injector and the spark plug as well as the exhaust side is relatively lean. The 120°CA BTDC case shows a more even distribution with richer mixtures close to the spark plug; however, the area around the exhaust valves still shows very lean mixtures. Finally, the 100°CA BTDC case shows zones with stoichiometric mixtures in the quenching zones around the entire combustion chamber. Consequently less hydrogen is available in the area around the spark plug. This suggests that the SOI 100 case might be difficult to experimentally evaluate due to the possible absence of ignitable mixtures around the spark plug, which leads to misfire. In addition, large areas in the combustion chamber dome close to the walls exhibit rich mixtures. Comparing these images it can be concluded that for the SOI 120°CA BTDC case hydrogen-rich zones are relatively isolated from the combustion chamber walls. Since wall heat transfer and thus wall heat losses increase with combustion gas proximity to the chamber walls, such stratification away from the walls is expected to have advantages in terms of wall heat losses.

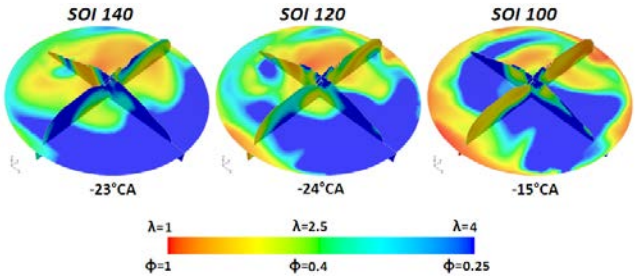


**Figure 7: Mixture distribution at ignition timing (SOI sweep, 5-hole nozzle)**

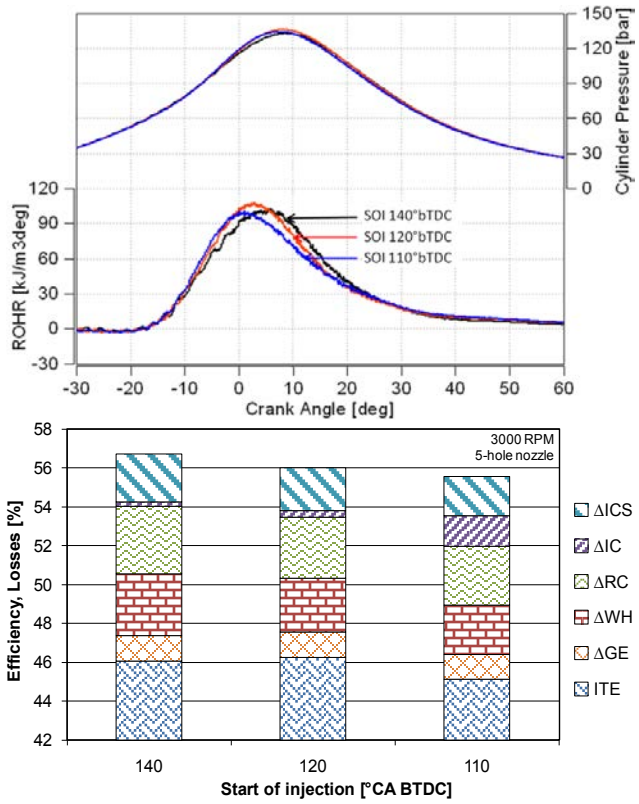


**Figure 8: In-cylinder pressure and rate of heat release (ROHR) curves (top) and analysis of losses (bottom) for three SOI timings with the 5-hole nozzle**

Both high speed in-cylinder pressure and rate of heat release (ROHR) curves as a function of engine crank angle for the SOI sweep with the 5-hole injector are shown in Figure 8. As predicted by the simulation results, stable combustion at an SOI of 100°CA BTDC could not be maintained. Thus the experimental results include SOI 140, 120 and 110°CA BTDC. Little difference can be seen in the pressure traces but there is a noticeable difference in ROHR. The first interesting observation is that rate of heat release during the early phase of combustion is faster with later SOI. As suggested by the 3D-CFD results this

can be attributed to a stronger mixture stratification resulting in higher flame speeds of the richer mixture clouds. The corresponding analysis of losses for the SOI sweep shows an efficiency of the ideal engine with real charge in the range of around 56%. The differences stem from slight changes in fuel and air mass and thus resulting air fuel ratio. As expected the losses due to injection during the compression stroke (ΔICS) decrease with later start of injection. The benefit of a decreasing ΔICS is offset in the SOI 110°CA BTDC case by increased losses due to incomplete combustion (ΔIC). This is partly due to more $H_2$ trapped in the quenching zone as suggested in the CFD results. As mentioned above the engine could not be operated at SOI 100°CA BTDC.

In summary, the 5-hole nozzle performs best at SOI 120°CA BTDC. At this condition the combustion phasing with a 50% MFB location at 8.2°CA ATDC is ideal while the combustion duration (90% MFB-10% MFB) of 52°CA is relatively slow compared to the other nozzles. This can be attributed to a more homogeneous mixture with leaner zones around the spark plug compared to the other nozzle designs. The difference between ideal constant volume combustion at TDC and real combustion (ΔRC) amounts to a 3.2% loss in efficiency. In terms of wall heat losses (ΔWH), the mixture stratification at SOI 120°CA BTDC is favorable which provides a relatively low ΔWH value of 2.8%. This is the primary benefit of using the 5-hole nozzle.

13-hole nozzle

With more holes one would expect the 13-hole nozzle to spread hydrogen throughout the combustion chamber and lead to a more homogeneous mixture at ignition timing. This is not the case, due the jet-to-jet interaction where the 13 jets merge into a single jet immediately downstream of the nozzle (see Figure 5). Mixture stratification with the 13-hole nozzle, shown in Figure 9, is similar for SOI 140 and 120°CA BTDC with the main difference being a more centralized mixture with later SOI. For SOI 100°CA BTDC the mixture stratification is similar to that for the 5-hole nozzle with hydrogen clouds in the quenching zone. Likewise one would expect issues with combustion stability for this case. The CFD results show an SOI 100°CA BTDC case for which the experimental assessment could not be completed due to combustion instabilities. For this reason the experimental results shown are for SOI 105°CA BTDC.

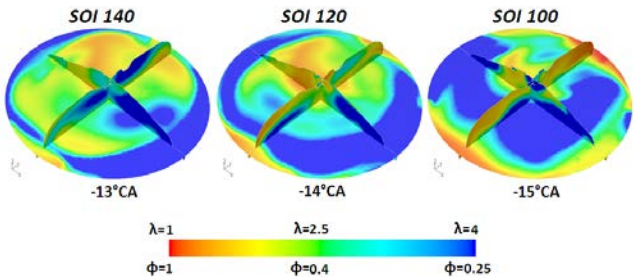


**Figure 9: Mixture distribution at ignition timing (SOI sweep, 13-hole nozzle)**

Pressure traces and rates of heat release for the SOI 140°CA BTDC and 120°CA BTDC are almost identical both in terms of shape and peak values. The SOI 105°CA BTDC case shows significantly lower peak pressures caused by slower heat release. This corresponds well with the CFD results suggesting that leaner mixtures are present around the spark plug and hydrogen rich areas are in the quenching zones which cause the delayed combustion. Combustion phasing is usually controlled by ignition timing but in this case it was also constrained by the availability of ignitable mixtures near the spark plug. The 50% MFB in this late SOI case is 17°CA ATDC which is far from the ideal phasing (Figure 10, top).

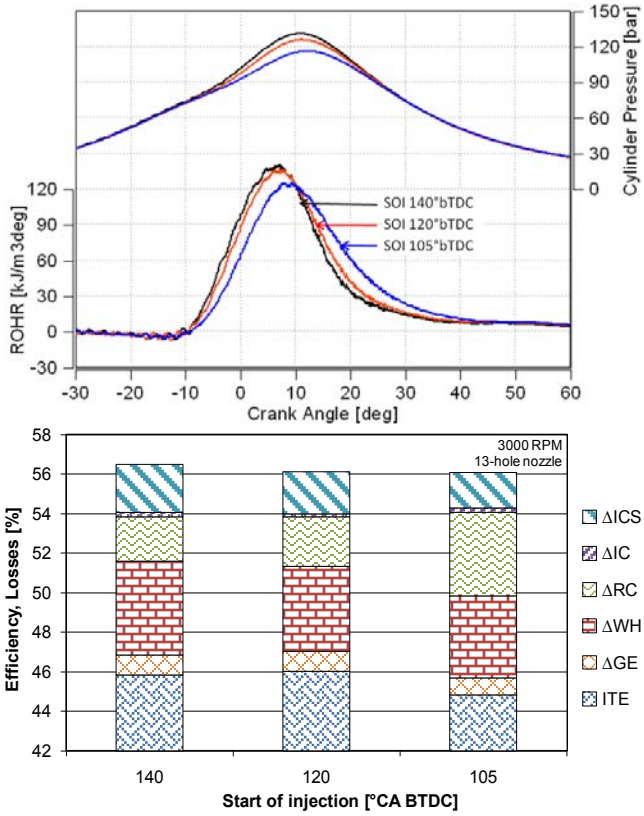


**Figure 10: In-cylinder pressure and rate of heat release (ROHR) curves (top) and analysis of losses (bottom) for three SOI timings with the 13-hole nozzle**

For all three injection timings the analysis of losses (Figure 10, bottom) starts from an efficiency of the ideal engine with real charge around 56%. As expected the losses due to injection during the compression stroke decrease with later SOI from 2.4% for the SOI 140°CA BTDC case to 1.8% with SOI 105°CA BTDC. Minimal differences in losses due to incomplete combustion ΔIC are observed. However, losses due to real combustion ΔRC almost double from 2.3% at SOI 140°CA BTDC to 4.2% at SOI 105°CA BTDC which can be attributed to the slower combustion and late phasing. At SOI 140 and 120°CA BTDC, the heat release is similar with a 50% MFB location around 10°CA ATDC. These two cases are also similar in terms of ΔRC and ΔWH. The main difference between these two cases is simply the SOI timing and resulting ΔICS. The 13-hole nozzle at SOI 120°CA BTDC has an ITE of 46.0%, 0.2% better than SOI 140°CA BTDC.

2-hole nozzle

As a result of the lower number of jets and inverse mixture formation strategy, with the jets impinging on the cylinder walls before being redirected by the piston, the 2-hole nozzle results in a different stratification than the other nozzles. The CFD results in Figure 11 show that the SOI 140°CA BTDC case results in a fairly rich mixture localized on the intake side; however, hydrogen rich areas also extend into the quenching zones. The amount of hydrogen in the quenching zones is reduced with SOI 100°CA BTDC while the stratification remains similar to the earlier case. Even for SOI 100°CA BTDC the mixture is stratified around the spark plug and unlike with the other nozzles, the engine operation was stable for this relatively late SOI case. Experimental results actually showed that stable operation was sustainable with injection as late as SOI 80°CA BTDC.

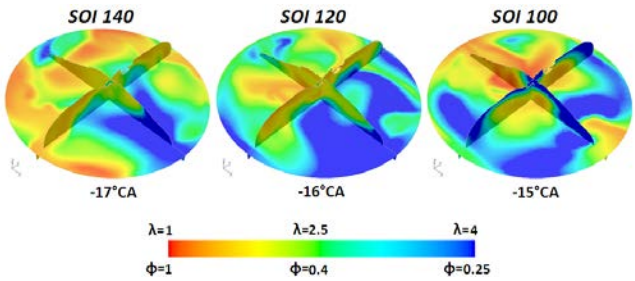


**Figure 11: Mixture distribution at ignition timing (SOI sweep, 2-hole nozzle)**

Experimental data also suggests a more stratified mixture resulting from the 2-hole nozzle (Figure 12, top) and confirms the conclusions drawn from the CFD results. Later start of injection results in a faster initial heat release rate as can be seen when comparing the ROHR curves for the SOI 140, 120 and 100°CA BTDC cases. This trend is similar to the one observed with the 5-hole nozzle and can again be attributed to richer $H_2$ clouds as a result of less time for mixing. Although stable combustion could be sustained for the SOI 80°CA BTDC case the heat release rate suggests disadvantageous stratification since both, the initial heat release rate is slower with a lower peak and more fuel is burned late in the cycle. The loss analysis (Figure 12, bottom) clearly shows the advantage of the late SOI reflected in reduced losses due to injection during the compression stroke ΔICS; 1.5% for 80°CA BTDC compared to 2.6% for the earliest injection (SOI 140°CA BTDC). However, the disadvantageous stratification for SOI 80°CA BTDC results in greatly increased losses due to real combustion ΔRC compared to the other cases. Finally, in all cases increased wall heat losses compared to other nozzle designs can be observed which is due to hydrogen rich clouds near the combustion chamber walls (see Figure 11). Overall the SOI 100°CA BTDC case with the 2-hole nozzle shows the highest indicated efficiency of 46.2%.

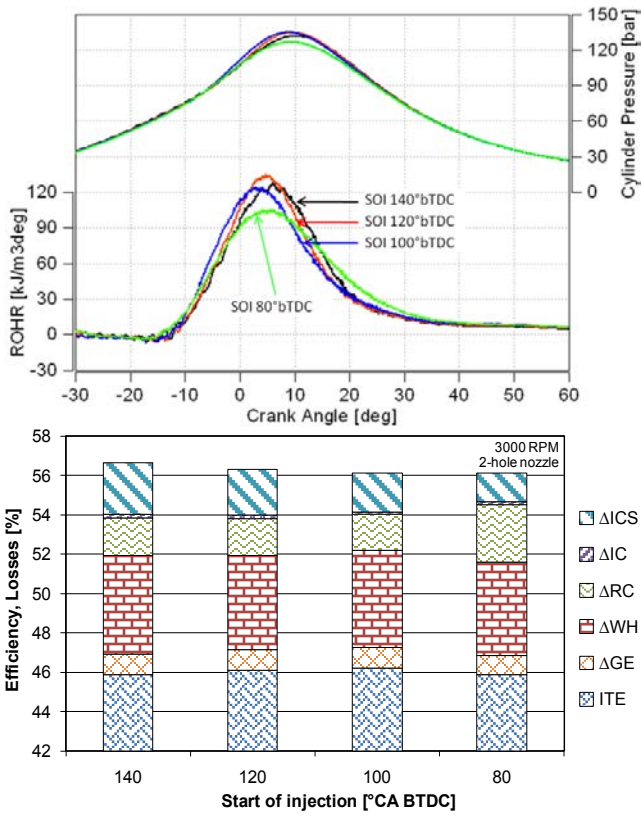


**Figure 12: In-cylinder pressure and rate of heat release (ROHR) curves (top) and analysis of losses (bottom) for four SOI timings with the 2-hole nozzle**

The efficiency and emissions trends for the SOI sweeps with the 3 different nozzle designs are summarized in Figure 13. With the earliest injection starting at 140°CA BTDC indicated efficiencies of 45.8% and 46.1% and $NO_X$ emissions of approximately 150 ppm were achieved and the differences between the individual nozzles are marginal. Delaying the injection by 20°CA shows a slight efficiency improvement for all nozzle designs which is mainly attributable to the reduced losses due to injection during the compression stroke. Both, 2 and 13-hole nozzle also show little effect on $NO_X$ whereas emissions with the 5-hole nozzle increase by more than 30%. The trend continues to 100°CA BTDC for the 2-hole nozzle where we see a peak ITE of over 46.2%. With this relatively late timing, neither the 5-hole nor the 13-hole nozzle provides stable combustion and the SOI sweep shows dropping efficiency even at earlier SOI. For both nozzles peak efficiency is observed at SOI 120°CA BTDC. Despite an earlier optimal SOI, the peak ITE of 46.3% for this operating condition is achieved with the 5-hole nozzle, however, the stratification also results in a $NO_X$ value of 217 ppm. On the other hand, the 2-hole nozzle achieves an almost identical efficiency with a later SOI at only 140 ppm $NO_X$ emissions. These differences in $NO_X$ emissions are caused by the distinct mixture stratifications stemming from the nozzle design. The CFD results for the 2-hole nozzle (Figure 10) show very lean and very rich zones in the combustion chamber. Applying the $NO_X$ trend for varying equivalence ratio (Figure 2), there is a peak around λ=1.3 and $NO_X$ emissions decrease for both leaner and richer mixtures. Ideal mixture stratification is therefore both rich and lean while avoiding conditions

conducive to $NO_X$ formation which appears to be best accomplished with the 2-hole nozzle correlated to lower $NO_X$ values (Figure 13).

A comparative analysis of nozzles for the most efficient SOI case for each injector nozzle design is also shown in Figure 13. As mentioned earlier the corresponding SOI is 120°CA BTDC for the 5-hole and 13-hole nozzle and 100°CA BTDC for the 2-hole nozzle. In all cases the efficiency of the ideal engine with real charge is around 56%. The later SOI for the 2-hole nozzle results in reduced losses due to injection during the compression stroke ΔICS. Losses due to incomplete combustion ΔIC at these operating conditions are marginal for all nozzles. The stronger stratification resulting from the 2-hole nozzle design as well as the later SOI results in a faster combustion which reduces losses due to real combustion process ΔRC. However, the stronger stratification also results in increased wall heat losses ΔWH. Finally, gas exchange losses ΔGE are comparable resulting in the indicated efficiencies stated above.

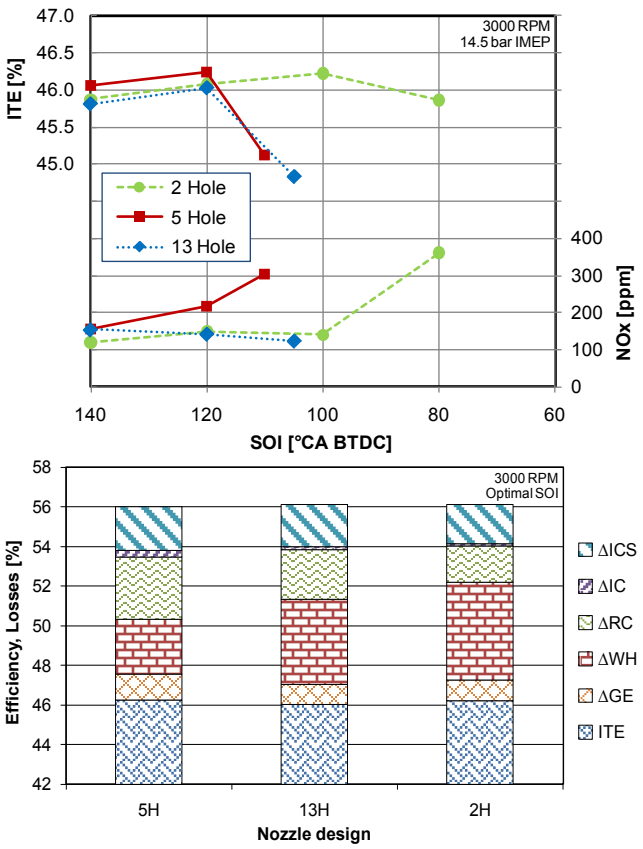


**Figure 13: Influence of SOI on indicated efficiency and $NO_X$ emissions (top) and comparative analysis of losses (bottom) for the three nozzles at 3000 RPM**

Comparing the results for the 3 nozzle designs it can be concluded that the trends in mixture stratification and engine performance are consistent with the concept of ideal mixture stratification. The 5-hole nozzle performs better in terms of ITE because an ignitable mixture near the spark plug is formed such that combustion phasing can be optimized and the mixture is relatively isolated from the combustion chamber walls. The downside of the 5-hole nozzle is that it runs the risk of $NO_X$ emissions in excess of 200 ppm which is more than the other nozzles and this is likely due to a slightly less stratified mixture. The 2-hole nozzle provides a very rich mixture that is close to the combustion chamber walls resulting in increased losses associated with mixture stratification. It is still able to achieve almost the same efficiency as the 5-hole nozzle mainly because it provides stable combustion conditions for a further delayed SOI which has the benefit of decreased losses due to injection during compression.

The actual friction losses of a single-cylinder engine are not representative of typical automotive multi-cylinder engines. Factors increasing friction of a research engine compared to production engines include the rigid design, balancing mechanism and the fact that all friction is attributed to a single cylinder. Instead of using actual friction data from the single-cylinder engine, friction losses were estimated based on friction data of a friction-optimized multi-cylinder engine. Assuming a friction mean effective pressure (FMEP) of 0.7 bar at the high load conditions at 3000 RPM results in friction losses in the range of 2.2% and a maximum brake thermal (BTE) efficiency at these operating conditions in excess of 44%.

## EFFECT OF ENGINE SPEED

The operating conditions at 3000 RPM with simulated turbocharging present a challenge in terms of mixture stratification because of the short time available for mixture formation and were therefore chosen for the exploration of both experimental and CFD results. Since mixture formation is a time dependent phenomenon, it is also interesting to consider the effect of engine speed on the performance of the three different nozzles. SOI sweeps, similar to those at 3000 RPM, were also performed at 2500 and 2000 RPM.

The indicated efficiency and $NO_X$ emissions results for the SOI sweep at 2500 RPM are summarized in Figure 14. The trends are similar to the 3000 RPM case with increasing efficiencies at later SOI. As observed earlier late SOI is limited by stable operation which is a function of availability of ignitable mixtures around the spark plug. It is interesting to note that the peak efficiency case for each nozzle is shifted by 20°CA compared to the 3000 RPM case. This is due to the fact that the time allowed for mixture formation is similar and will positively influence the losses due to injection during the compression stroke ΔICS. Overall the peak efficiency values increase to 46.1% with the 13-hole nozzle, 46.2% with the 2-hole nozzle, and 46.7% with the 5-hole nozzle. It is further interesting to note that the efficiency increase is greater for the 5-hole nozzle compared to the other nozzles. This is likely a function of wall heat losses ΔWH because at lower speeds there is more time for heat transfer and, as previously seen, the combustion with the 5-hole nozzle exhibited lower wall heat losses due to favorable mixture stratification. In terms of $NO_X$ emissions the 2-hole nozzle is superior compared to the other nozzles. Even at the highest efficiency conditions for this nozzle (SOI 80°CA BTDC) $NO_X$

emissions values are lower than those for the other nozzles at any tested start of injection.

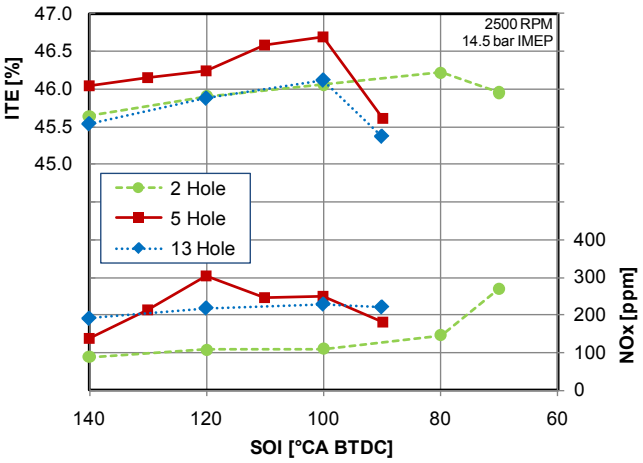


**Figure 14: Influence of SOI on indicated efficiency and $NO_X$ emissions for different nozzles at 2500 RPM**

A similar trend with peak efficiencies being achieved at later SOI continues for 2000 RPM (Figure 15). The highest efficiencies for the 2-hole and 13-hole are realized at SOI 80°CA BTDC with 46.1% and 46.3% respectively whereas the 5-hole nozzle efficiency peaks at SOI 90°CA BTDC with an ITE of 46.9%. While the efficiency drops significantly due to unstable combustion when further delaying SOI with the 5-hole and 13-hole nozzle, high engine efficiencies can be maintained even at SOI 60°CA BTDC with the 2-hole nozzle. However, the $NO_X$ emissions at this operating point increase to more than 230 ppm relative to less than 70 ppm for the SOI 80°CA BTDC case.

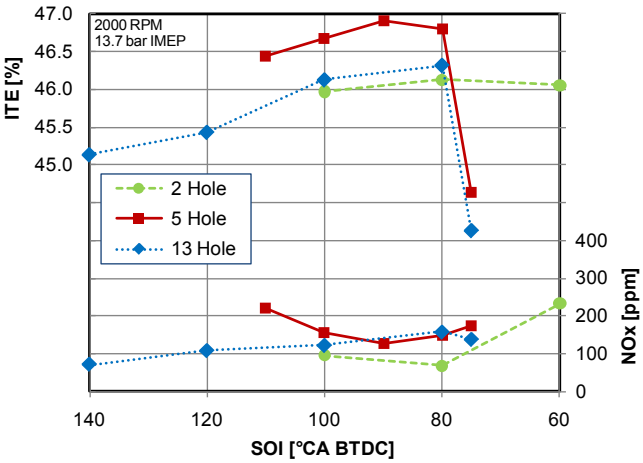


**Figure 15: Influence of SOI on indicated efficiency and $NO_X$ emissions for different nozzles at 2000 RPM**

In terms of the $NO_X$ target, the 2-hole nozzle is most promising because it provides a highly stratified mixture that is simultaneously lean and rich enough to avoid the $NO_X$ critical area around $\lambda = 1.3$ (as seen in the homogeneous $NO_X$ trend in Figure 2). Such stratification was observed for the 2-hole nozzle at 3000 RPM correlating to lower $NO_X$ emissions, a trend that continues for both 2500 and 2000 RPM. It may be possible to achieve the same benefit in terms of $NO_X$ emissions with the efficient 5-hole injector in future work by further optimizing the injection strategy. Possible options include multiple injections where a primary injection produces a stratified mixture based on the knowledge from this study and an additional late injection produces a rich cloud near the spark plug. Ongoing work also investigates the potential of optimizing the nozzle design such that a further delay in SOI can be accomplished without compromising combustion stability. Aside from optimizing the injection strategy itself, exhaust gas recirculation (EGR) has also been identified in a previous study as an effective measure to further reduce $NO_X$ emissions with little negative impact on engine efficiency [13].

As outlined earlier, an estimated brake thermal efficiency in excess of 44% was achieved at 3000 RPM based on friction assumptions of a multi-cylinder engine. It was also shown that reducing engine speed resulted in a further improvement in ITE from 46.3% at 3000 RPM to 46.7% at 2500 RPM up to 46.9% at 2000 RPM. Applying the same considerations in terms of engine friction and considering reduced FMEP with reduced engine speeds results in an estimated brake thermal of 44.7% at 2500 RPM and 45.0% at 2000 RPM.

## INFLUENCE OF INJECTION PRESSURE

The analyses of different nozzle designs as well as the assessment of the influence of engine speed clearly show that a later start of injection is desirable to improve the engine efficiency. In an attempt to quantify the benefits of further delaying the SOI with the current nozzle design, the effect of increased injection pressure was analyzed. Increasing injection pressure increases gas density and thus increases the injector mass flow. The same hydrogen mass can be injected in a shorter time period. For this limited set of tests an SOI sweep was performed with the 5-hole nozzle at an increased injection pressure of 140 bar. This increase in pressure from the baseline case with 100 bar injection pressure allows for a reduction in injection duration from 35°CA to approx. 25°CA (2000 RPM, full load). Considering just the effect of decreasing the injection duration, with the same SOI, losses due to injection during compression will increase. In this case, however, we will see a benefit in terms of SOI.

The effect of increased pressure on indicated thermal efficiencies and $NO_X$ emissions is summarized in Figure 16. The efficiency curve for the 140 bar case is shifted towards later SOI by approx. 10°CA. Given that this shift is equivalent to the reduction in injection duration, it appears that the end of injection is most critical for determining at which injection timings stable operating conditions can be maintained. It can be seen from the results in Figure 16 that the efficiency improvement due to later SOI outweighs the slightly increased losses due to injection duration, except for SOI 100°CA BTDC. In terms of $NO_X$ emissions the same shift by approx. 10°CA can be observed without influencing the absolute emissions level.

Figure 16 also shows the analysis of losses for the highest ITE operating conditions at 100 and 140 bar. These are achieved at an SOI of 90°CA BTDC with the lower injection pressure and SOI 80°CA BTDC

with the increased pressure. The more optimal later SOI at 140 bar injection pressure results in a slight reduction in losses due to injection during the compression stroke ΔICS. With the losses due to incomplete combustion, real combustion, wall heat and gas exchange practically identical, the higher injection pressure results in an indicated efficiency of 47.1%. Using the same friction assumptions as outlined in the analysis of engine speed suggests that by increasing the injection pressure with the 5-hole nozzle an estimated BTE in excess of 45.1% can be achieved, which exceeds the DOE efficiency target.

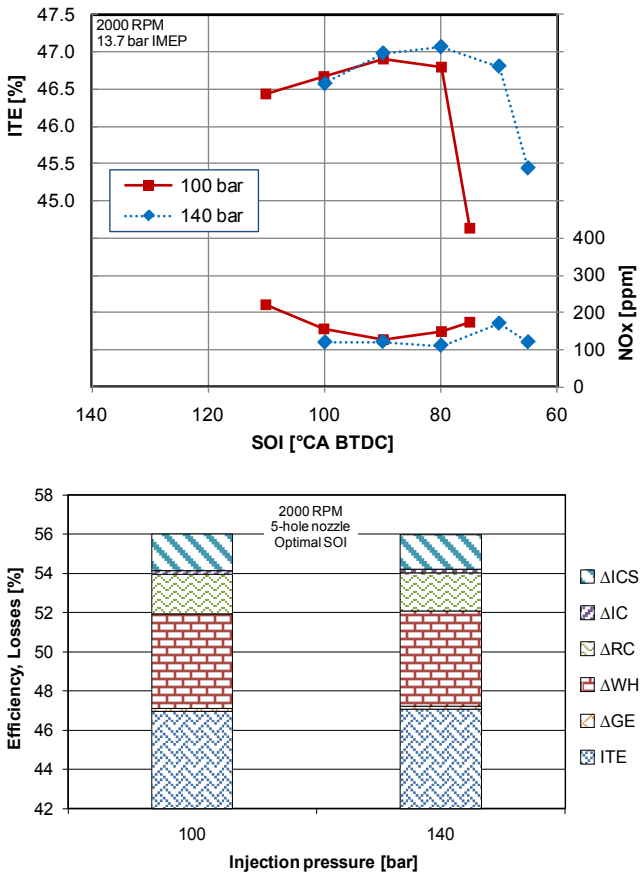


**Figure 16: Influence of increased injection pressure on engine efficiency and $NO_X$ emissions (top) and comparative analysis of losses (bottom) at 2000 RPM with the 5-hole nozzle**

## CONCLUSIONS

Hydrogen internal combustion engines are considered a promising technological solution to reduce pollutant formation while ensuring power densities comparable to conventional (gasoline) engines. This paper shows the promising potential of direct injection of hydrogen to meet the targets set by the U.S. DOE in terms of efficiency and $NO_X$ emissions. Direct injection provides many degrees of freedom for optimizing the injection strategy to minimize individual losses and $NO_X$ emissions.

This paper analyzes the influence of operational (SOI) and geometrical (nozzle design) parameters on ITE and $NO_X$ emissions on a single-cylinder research engine fuelled by direct injection of hydrogen. Three nozzles, providing different injection and mixture formation strategies, are initially tested at 3000 RPM and 14.5 bar IMEP, the most challenging and critical operating conditions for $NO_X$ emissions. An analysis of losses is carried out to highlight the contribution of the major factors affecting the indicated thermal efficiency. CFD simulations are performed to gain insight into the in-cylinder processes and provide further understanding of the experimental results.

Results show that for the 5-hole and 13-hole nozzle the optimum injection timing at 3000 RPM is SOI 120°CA BTDC. Earlier injection was found to require more compression work and provides mixtures which are not properly stratified around the spark plug. Later injection did not provide sufficient time for the fuel jet to reach the spark plug after impinging the cylinder walls and led to unstable combustion, characterized by high COV of IMEP. Similar results were observed for the 2-hole nozzle but with a broader operating range and an optimal SOI at 100°CA BTDC.

At lower speeds the engine efficiency was expected to decrease due to higher wall heat losses. Nevertheless, the increased time at lower speed for the fuel jet to imping the walls and stratify around the spark plug allowed for a further delay of the start of injection. Accordingly, the compression work could be reduced and in some cases the efficiency increased. The 5-hole nozzle, which exhibits the lowest wall heat losses, showed the highest efficiency of 46.9% at 2000 RPM with an SOI of 90°CA BTDC. Furthermore, the friction losses decrease at a lower engine speed and an estimation suggests that a brake thermal efficiency of 44.9% could be achieved with a multi-cylinder engine. Finally, increasing the injection pressure from 100 to 140 bar allowed for another 10°CA delay in SOI and thus for a slight reduction in losses due to injection during the compression stroke. With a measured indicated thermal efficiency of 47.1% the estimated brake thermal efficiency for these operating conditions reaches 45.1% and thus also exceeds the DOE efficiency target of 45%.

$NO_X$ emissions need to be evaluated on an entire drive cycle. Typical values reported in this study are around 200 ppm. At the peak indicated efficiency conditions the corresponding $NO_X$ emissions were only slightly higher than 100 ppm. Further, the high load operating conditions analyzed in this study are certainly the most severe in terms of $NO_X$ emissions since at lower engine loads typical for drive cycle operation the average air fuel ratio would be leaner suggesting lower $NO_X$ emissions.

## ACKNOWLEDGMENTS

The submitted manuscript has been created by UChicago Argonne, LLC, Operator of Argonne National Laboratory ("Argonne"). Argonne, a U.S. Department of Energy Office of Science laboratory, is operated under Contract No. DE-AC02-06CH11357. The U.S. Government retains for itself, and others acting on its behalf, a paid-up nonexclusive, irrevocable worldwide license in said article to reproduce, prepare derivative works, distribute copies to the public, and perform publicly and display publicly, by or on behalf of the Government.

This research was funded by DOE's FreedomCAR and Vehicle Technologies Program, Office of Energy Efficiency and Renewable Energy. The authors wish to thank Gurpreet Singh, program manager at DOE, for his support. The hydrogen engine used to run these experiments was provided by Ford Motor Company. Special thanks to Brad Boyer and his team from Ford Motor Company for their support.

Graphs showing crank-angle resolved data were created and calculations of heat release rate were performed using AVL Concerto. The authors wish to express their gratitude to staff at AVL North America Inc. and AVL List GmbH Austria for their support.

## REFERENCES

1 S. Verhelst, R. Sierens, "A Critical Review of Experimental Research on Hydrogen Fueled SI Engines", SAE Technical Paper 2006-01-0430, 2006.
2 C. M. White, R. R. Steeper, A. E. Lutz, "The hydrogen-fueled internal combustion engine: a technical review". Int. J. Hydrogen Energy 31:1292-1305, 2006.
3 S. Verhelst, T. Wallner, "Hydrogen-fueled internal combustion engines", Progress in Energy and Combustion Science, Volume 35, Issue 6, Pages 490-527, 2009.
4 A. Wimmer, T. Wallner, J. Ringler, F. Gerbig, "H2-Direct Injection - A Highly Promising Combustion Concept", SAE Technical Paper 2005-01-0108, 2005.
5 U.S. Department of Energy, FreedomCAR and Fuel Technical Partnership Technical Goals, Washington, D.C, 2002.
6 T. Wallner, A. M. Nande, J. Naber, "Evaluation of Injector Location and Nozzle Design in a Direct-Injection Hydrogen Research Engine", SAE Technical Paper 2008-01-1785, 2008.
7 T. Wallner, R. Scarcelli, A. M. Nande, J. Naber, "Assessment of Multiple Injection Strategies in a Direct Injection Hydrogen Research Engine", SAE Technical Paper 2009-01-1920, 2009.
8 H. Obermair, R. Scarcelli, T. Wallner, "Efficiency Improved Combustion System for Hydrogen Direct Injection Operation", SAE Technical Paper 2010-01-2170, 2010.
9 T. Wallner, "Development of combustion concepts for a hydrogen powered internal combustion engine", PhD thesis, Graz University of Technology, 2004.
10 R. Scarcelli, T. Wallner, V.M. Salazar, S.A. Kaiser, "CFD and Optical Investigations of Fluid Dynamics and Mixture Formation in a DI-H2 ICE", presented at ASME ICEF Conference 2010, ASME Paper ICEF2010-35084, 2010.
11 R. Scarcelli, T. Wallner, N. Matthias, V.M. Salazar, S.A. Kaiser, "Numerical and Optical Evolution of Gaseous Jets in Direct Injection Hydrogen Engines", SAE Technical Paper 2011-01-0675, 2011.
12 Tritton, D.J., Physical Fluid Dynamics, Van Nostrand Reinhold, 1977 (reprinted 1980), Section 22.7, The Coanda Effect.
13 T. Wallner, A. Nande, R. Scarcelli, "Evaluation of exhaust gas recirculation (EGR) in combination with direct injection (DI) on a Hydrogen Research Engine", World Hydrogen Technology Convention, New Delhi/India. 2009.

## CONTACT

Thomas Wallner, Ph.D.
Argonne National Laboratory
Energy Systems Division
Building 362
9700 South Cass Avenue
Argonne, IL 60439-4815
Phone: 630.252.3003
Cell: 312.933.4602
Fax: 630.252.3443
Email: twallner@anl.gov

## DEFINITIONS, ACRONYMS, ABBREVIATIONS

| | |
|---|---|
| **ABDC** | After Bottom Dead Center |
| **ATDC** | After Top Dead Center |
| **BBDC** | Before Bottom Dead Center |
| **BTDC** | Before Top Dead Center |
| **BTE** | Brake Thermal Efficiency |
| **°CA** | Degree Crank Angle |
| **CFD** | Computational Fluid Dynamics |
| **COV** | Coefficient of Variation |
| **DI** | Direct Injection |
| **DOE** | Department of Energy |
| **EVC** | Exhaust Valve Closing |
| **EVO** | Exhaust Valve Opening |
| **$H_2$** | Hydrogen |
| **ICE** | Internal Combustion Engine |
| **IMEP** | Indicated Mean Effective Pressure |
| **ITE** | Indicated Thermal Efficiency |
| **IVC** | Intake Valve Closing |
| **IVO** | Intake Valve Opening |
| **MBT** | Maximum brake torque |
| **MFB** | Mass fraction burned |
| **$NO_X$** | Nitrogen Oxides |
| **PIV** | Particle Imaging Velocimetry |
| **PFI** | Port Fuel Injection |
| **ROHR** | Rate of Heat Release |
| **RPM** | Revolution per Minute |
| **SOI** | Start of Injection |
| **TDC** | Top Dead Center |
| **Ma** | Mach number |
| $\phi$ | Equivalence ratio |
| $\lambda$ | Air fuel ratio |
| $\eta_{IRC}$ | Efficiency of ideal engine with real charge |